

Experimental Investigation of Transitional Free Shear Layer Optics

Larry Chew*

University of Central Florida, Orlando, Florida 32816
and

Walter Christiansen†

University of Washington, Seattle, Washington 98195

Measurements of Strehl ratio vs downstream distance, when a beam propagates through a shear layer (Reynolds number = 810/length), reveal minimal phase distortion in the pretransition region and a sudden decrease in the Strehl ratio when transition occurs. The Strehl ratio levels off to a constant asymptotic value (which is a function of the velocity ratio) in the post-transition region. The constant Strehl ratio (in the fully developed region) is attributed to fast mixing that occurs within the core of the vortices. Measurements in the post-transition region show that the Strehl ratio takes a U-shape profile when the velocity ratio is varied from 0.4 to 0.8. Results of mathematical simulation show that coherent structures may be modeled as a sinusoidal phase plate.

Nomenclature

$B(x)$	= amplitude of the sinusoidal wave
b	= Gadstone-Dale constant
D	= beam diameter
d	= vortex size
f_0	= frequency of the sine function
J_q	= Bessel function of the first kind, order q
k	= wave number = $2\pi/\lambda$
l	= path of beam travel
l_x	= width of the aperture in the x_1 direction
l_y	= height of the aperture in the y_1 direction
m	= peak-to-peak excursion of the phase delay
n	= refractive index
n_1	= refractive index, one shear-layer stream
n_2	= refractive index, the second shear-layer stream
$t(x_1, y_1)$	= transmittance function
$U(x_1, y_1)$	= near-field electric field strength
$U(x_0, y_0)$	= far-field electric field strength
U_1	= fluid velocity of upper stream
U_2	= fluid velocity of lower stream
x	= downstream distance from splitter plate
x_0, y_0	= observation plane
x_1, y_1	= aperture plane
z	= distance between aperture plane and observation plane
α	= constant of proportionality
Δ	= shear-layer interface
δ	= shear-layer thickness
ζ	= phase factor
θ	= angle of the coordinate plane to the aperture
Λ	= integral length scale of turbulence
λ	= wavelength
λ_0	= density ratio
ρ	= fluid density
ρ_1	= fluid density of upper stream
ρ_2	= fluid density of lower stream
σ_Φ^2	= variance of the phase variation

Φ	= wave aberration
$\phi(x)$	= phase excursion
ρ	= nondimensionalized radius of the Gaussian sphere
$\langle \rangle$	= spatial average

I. Introduction

THE study of refractive scattering by turbulent shear flows has become important due to interest in imaging systems and application of laser.¹ In such applications, a laser beam is propagated through a shear layer (see Fig. 1) and if such a shear layer consists of fluids with different refractive indices, then random phase variations can be produced in the beam (even at low speed), thereby causing a reduction of the beam intensity.² For applications such as laser propagation through the atmosphere, laser targeting, and camera/telescope cavity,^{3,4} such losses in beam intensity are undesirable, and therefore it is important to understand the effects of shear-layer turbulence on laser propagation.

Numerous studies have been conducted on this subject and a detailed overview of current literature is described in Ref. 5. It is important at this point to reiterate that most of the previous studies on laser propagation through a turbulent medium assume homogeneous turbulence. Brown and Roshko⁶ showed that shear-layer turbulence is not purely homogeneous, but instead consists of large-scale vortices called coherent structures. The effects of these coherent structures on laser propa-

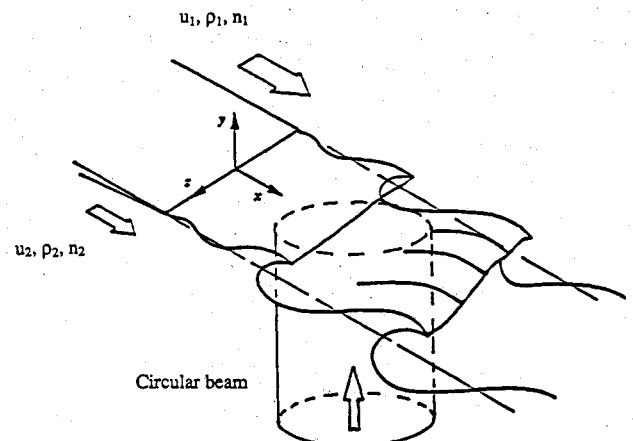


Fig. 1 Laser beam passing through a shear layer.

Received Feb. 11, 1992; revision received March 8, 1993; accepted for publication March 8, 1993. Copyright © 1993 by the American Institute of Aeronautics and Astronautics, Inc. All rights reserved.

*Assistant Professor, Department of Mechanical and Aerospace Engineering, Member AIAA.

†Professor, Department of Aeronautics and Astronautics, Associate Fellow AIAA.

gation are presented in Ref. 7 and a summary of the paper is as follows: An experimental facility was constructed in which a shear layer was generated using air and a mixture of helium/argon having the same density as air. A helium/neon laser beam (6328 Å) was propagated through the shear layer and the intensity of the beam was measured by a CCD camera. It was found that the intensity profile of the beam was determined by the coherent structures. The profile was not Gaussian but multiple-peaked, depending on the size and position of these large vortices relative to the beam position. Since the profile was determined by the coherent structures, controlling these structures allows for the possibility of controlling beam propagation. This was clearly demonstrated when the Strehl ratio (defined as the peak intensity ratio of a far-field measurement of a beam with phase distortion to that of a diffraction-limited beam) of a beam propagating through a perturbed shear layer was markedly larger than that through a shear layer that was not perturbed.

This paper is a continuing report on further progress in our research on shear-layer optics. The main focus of this research is to obtain a better understanding of the effects of coherent structures on laser propagation. Three sets of tests were conducted in this research. The first test proved that coherent structures affected the optics and the second test studied the effects of forcing a shear layer. The results of these two tests were reported in our initial paper (see Ref. 7). The third test (reported in this paper) studies the relationship between the shear-layer fluid mechanics and beam propagation quality. A beam is propagated through different sections of a shear layer to allow different-size vortices to affect the Strehl ratio. Correlation of Strehl ratio data vs laser position in the shear layer sheds some light on the influence of large vortices on laser propagation; these results and the discussion thereof are given in Sec. IV. A mathematical model is developed to explain the observed results and presented in Sec. V.

II. Theory Definition of Strehl Ratio

In a mixing layer, turbulence creates random spatial fluctuations in species concentration (mass density and temperature variation can occur as well). These variations correspond to fluctuations in the gas refractive index given by the Lorentz-Lorenz formula

$$n = 1 + K\rho \quad (1)$$

where $K = b/\rho_{\text{ref}}$ and b is the Gladstone-Dale constant.⁸ Fluctuations in refractive indices lead to phase distortion in the beam, resulting in loss of intensity. A common method of defining beam quality uses the Strehl ratio, a far-field diffraction intensity ratio. The tilt-corrected Strehl ratio (SR) is given by the following expression⁸:

$$\text{SR} \equiv -\frac{1}{\pi^2} \left| \int_0^1 \int_0^{2\pi} e^{i\Phi} \rho \, d\rho \, d\theta \right|^2 \quad (2)$$

where Φ is the wave aberration, ρ is the nondimensionalized radius of the Gaussian sphere, and θ is the angle of the coordinate plane to the aperture (see Ref. 8 for detailed mathematics). This expression defines the instantaneous Strehl ratio of a laser beam passing through any phase-distorting

medium. If the phase aberration is small, the SR may be approximated by the following empirical formula as shown by Mahajan⁹:

$$\text{SR} \approx e^{-\sigma_\Phi^2} \quad (3)$$

where σ_Φ^2 is called the variance of the phase variation. In 1969, Sutton¹⁰ modeled this variance to be

$$\sigma_\Phi^2 = 2k^2 \langle (\Delta n)^2 \rangle \Lambda \delta \quad (4)$$

where k is the wave number, n is the index, Λ is the integral length scale of turbulence, and δ is the thickness of the shear layer.

Applying these models to laser propagation through a shear layer and using mixing and volume fraction arguments, Vu et al.¹¹ showed that the final form of the Strehl ratio for a low-speed homogeneous shear layer between two optically dissimilar gases may be written as

$$\text{SR} = \exp \{ -2k^2 \alpha^2 (n_1 - n_2)^2 \delta^2 / 4 \} \quad (5)$$

where α is a constant of proportionality ($\alpha^2 = 0.15$) and $n_1 - n_2$ is the index difference between the two fluid streams. This model has been widely used as the means of predicting the Strehl ratio³ of a laser beam propagating through a shear layer. However, it should be stressed that this model is meant for a homogeneous fluctuating density field and therefore will not describe a naturally occurring shear layer accurately. Our experiments confirm this fact when results show that the Strehl ratio values did not match those obtained with Sutton's formulation. A shear layer therefore cannot be treated as a homogeneous field, but rather as one that consists of large-scale coherent structures.

III. Experimental Setup

A wind tunnel is built to generate a mixing layer consisting of two optically dissimilar gases. (See Ref. 5 to obtain a detailed description of tunnel construction.) The velocity ratio and density ratio of the shear layer can be varied independently. A test section (12 in. \times 4 in. \times 2 in.) is constructed of Plexiglas and has four optical windows (surface quality of $\lambda/8$) that allow for passage of the laser beam. The walls of the test section are adjusted to remove streamwise pressure gradient in the flow.

The source of external perturbation to the shear layer is a 10-mm-wide, 1-mm-thick oscillating plate attached to the trailing edge of the splitter plate. The plate is connected to two acoustic speakers driven at frequencies ranging from 0 to 350 Hz.

The optical apparatus passes a collimated beam (wavelength is 6328 Å) through a shear layer, and a receiving telescope focuses the resultant beam onto an image-acquisition camera. Two beam paths are formed by a 50/50 beam splitter; the first beam is directed through the shear layer, whereas the second beam is passed (at right angles to the first beam) through the layer and onto a photographic plate (to obtain side-view pictures of the shear layer at the same instant as the plan-view intensity profile). This laser shadowgraph system is used to study instantaneous vortex structures and their effects on the far-field beam intensity profile.

A CCD camera is used to capture either a 2-s (time-averaged) or 100- μ s (instantaneous) exposure image of the intensity profile. The ratio of the peak intensity of the beam with the shear layer turned onto that with the shear layer turned off determines the Strehl ratio. The results presented in this paper consist only of the long time exposure of 2 s (time-averaged).

In all experiments, the shear layer is generated using a helium/argon mixture as the slow stream (top stream) and air as the faster stream (bottom stream). Helium (30.6%) and argon (60.9%) are mixed to provide a density ratio of 1.0 with respect to air and refractive index difference ($\Delta n = 8.5 \times 10^{-5}$) between the two streams. At such low speeds, aerodynamically

Table 1 Initial conditions

Parameter	Value
$U_{\text{fast}}(\text{air})$	3.0 m/s
$U_{\text{slow}}(\text{He/Ar mixture})$	1.8 m/s
U_{average}	2.4 m/s
Velocity ratio u_u	0.6
Mixture volume ratio	He/Ar : 30.6/69.4%
Natural frequency	280 Hz
Laser wavelength λ	6328 Å
Index change Δn	8.54×10^{-5}
$Re/\text{length} (\rho_{\text{air}} \Delta U / \mu_{\text{air}})$	810/cm

induced density fluctuations are negligible. The index of refraction gradient comes from the different Gladstone-Dale constants of helium/argon and air. The initial conditions of the experiments are presented in Table 1.

Procedure

A laser beam is positioned along the centerline of the shear layer. Two beams are used: a 1.0-cm-diam beam and 6.5-cm-diam beam. The beams are positioned at 3.5 cm downstream from the splitter plate and the Strehl ratio is obtained at increments of 1 cm through 24 cm downstream of the splitter plate. This experiment is conducted for two time exposures: 100 μ s and 2 s. The experiment is initially conducted for a shear layer at a velocity ratio of 0.6 and later repeated for velocity ratios of 0.4, 0.5, 0.7, and 0.8.

IV. Results and Discussion

A. Time-Averaged Strehl Ratio vs Downstream Position

Figure 2 shows the time-averaged Strehl ratio plotted vs downstream position from the splitter plate for an unperturbed shear layer. The intensity is time-averaged over 2 s, during which time approximately 80–200 vortices have passed through the 6.5-cm-diam beam. The Strehl ratio is constant at 0.9 from $x = 4$ to 8.5 cm. It then decreases rapidly to a value of about 0.4 at $x = 18$ cm and remains constant from then on. It is interesting to note that the region of rapid Strehl ratio decrease corresponds closely to the region of transition in the shear layer. Transition in the shear layer occurs when small-scale vortices suddenly appear and there is a sudden increase in mixing. It is detected by visualizing the shear layer from the top view using the shadowgraph technique. At about 8.5 cm, the shadowgraph reveals many small-scale vortices, thereby indicating the position of transition.

When transition occurs, smaller-scale three-dimensional vortices are formed that scatter the beam to cause intensity reduction. This suggests that smaller-scale three-dimensional turbulence causes larger phase distortion to a beam than the larger-scale two-dimensional vortices.

The end of transition is determined from a shadowgraph image of the shear layer. At about 18 cm, the increase in spatial density of the number of vortices in the shadowgraph appears to level off. This stop in increase in the number of small vortices signifies the end of transition and thus the start of the post-transition region.

In this post-transition region, the Strehl ratio asymptotes to a constant value instead of decreasing to 0.0 (Vu et al.'s formulation shown as + + in Fig. 2). One would expect that as the shear layer becomes thicker, the difference in optical path length grows larger; the phase distortion increases, causing the intensity to decrease. This is not observed and such an anomaly is hypothesized to be a consequence of mixing within

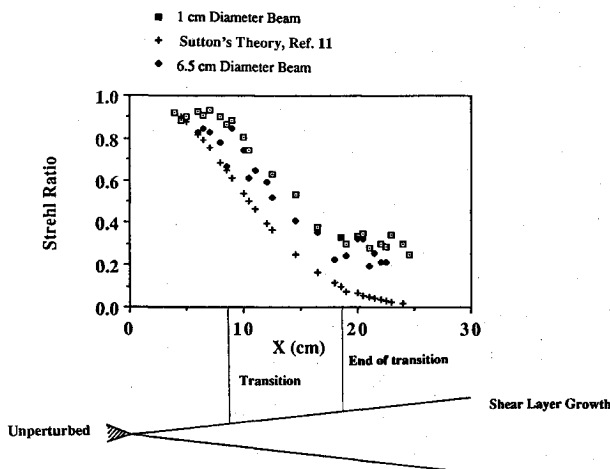


Fig. 2 Strehl ratio vs downstream position X .

Table 2 Flow conditions for five velocity ratios

Case	Velocity ratio λ_u	\bar{U} (m/s)	U_{fast} (m/s)	U_{slow} (m/s)	λ_p	δ/x
I	0.4	2.4	3.43	1.37	1.0	0.130
II	0.5	2.4	3.2	1.6	1.0	0.113
III	0.6	2.4	3.0	1.8	1.0	0.10
IV	0.7	2.4	2.82	1.98	1.0	0.091
V	0.8	2.4	2.67	2.13	1.0	0.057

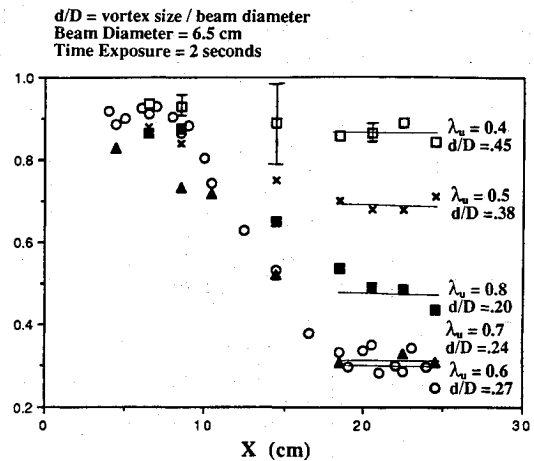


Fig. 3 Strehl ratio vs X for five velocity ratios.

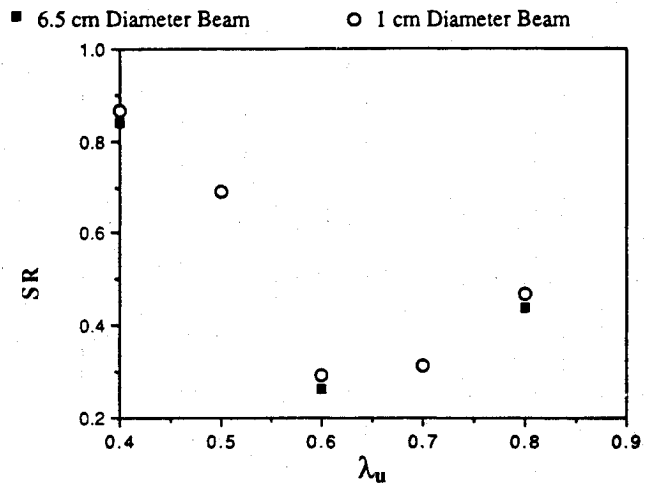


Fig. 4 Strehl ratio vs velocity ratio.

the large coherent structures (resulting in a uniform field inside the core of the vortices,¹² thereby causing phase distortion to be reduced). The effect of phase-error reduction cancels that of an increase in optical path length, resulting in a nearly constant Strehl ratio.

B. Effects of Growth Rate on Strehl Ratio

The effect of growth rates on the Strehl ratio is obtained by conducting the foregoing experiments on five shear layers with different velocity ratios. Table 2 presents the conditions of the five shear layers.

The plot of the Strehl ratio averaged over 2 s vs downstream position for each of these velocity ratios is shown in Fig. 3. The beams used in these experiments were 6.5 cm in diameter. In all cases, the Strehl ratio is constant at 0.9 for the first few centimeters (x less than 11 cm). The Strehl ratio then begins to fall off very quickly and asymptotes to five different values. Values of the asymptotic Strehl ratio are plotted vs the velocity ratio and illustrated in Fig. 4. The figure reveals that the

asymptotic Strehl ratio takes on a U-shaped form, contrary to what was initially expected. Since the Strehl ratio is a function of spatial phase error that was thought to be a linear function of shear-layer thickness, it was expected that as the shear layer became thicker, the Strehl ratio would decrease. However, this did not happen; the Strehl ratio did not monotonically decrease with increasing shear-layer thickness. This result is attributed to the large coherent structures behaving like a diffraction pattern (multiple slit diffraction grating), which causes a sinusoidal phase delay on the phase front. The new phase front can in fact interfere to cause an increase in the Strehl ratio. One good example that is analogous to the foregoing phenomenon is basic diffraction theory. In a physics laboratory, it is easy to demonstrate that under certain conditions, the diffraction pattern of light around an opaque circle is a bright central spot. The wavefront interferes to create a large intensity in the central region. Similarly, this happens when a shear layer behaves like a sinusoidal phase plate to cause constructive interference. The size of the vortices δ determines the wavelength of the grating. This model has been tested and is presented in Sec. V.

C. Strehl Ratio vs x for a Forced Shear Layer

Figure 5 shows the Strehl ratio (obtained with a 1-cm-diam beam) vs downstream position for an unperturbed and a perturbed shear layer. The perturbation was obtained by an oscillating flap at the tip of the splitter plate (see Ref. 5 for details of the experimental setup). In these experiments, the flap was oscillated at the natural frequency of the shear layer that was found by a hot-wire probe. The line formed by diamonds in the graph shows the Strehl ratio for a perturbed shear layer, whereas that formed by squares is for an unperturbed shear layer. All the values (every x position) of the perturbed shear-layer Strehl ratio are higher than those in the unperturbed case. In addition, the Strehl ratio at the upstream location remains constant over a longer length (until $x = 12.5$ cm) before it dramatically drops off in value. Shadowgraphs of the forced shear layer reveal that the additional region of constant and high Strehl ratio values coincides with the region in which the thickness of the shear layer remains constant. When the shear layer begins to grow linearly again, the Strehl ratio decreases in value. A 6.5-cm-diam beam gives data similar to those of the 1-cm-diam beam, but no relationship was found between the beam diameter and amount of Strehl ratio improvement.

D. Improvement in Strehl Ratio for a Forced Shear Layer

When the shear layer is forced at its natural frequency, an obvious difference is observed. The Strehl ratio remains high and constant from $x = 4$ cm to $x = 12$ cm. These additional 2 cm in which the Strehl ratio remains high correspond to the area where the shear layer stops growing and remains constant

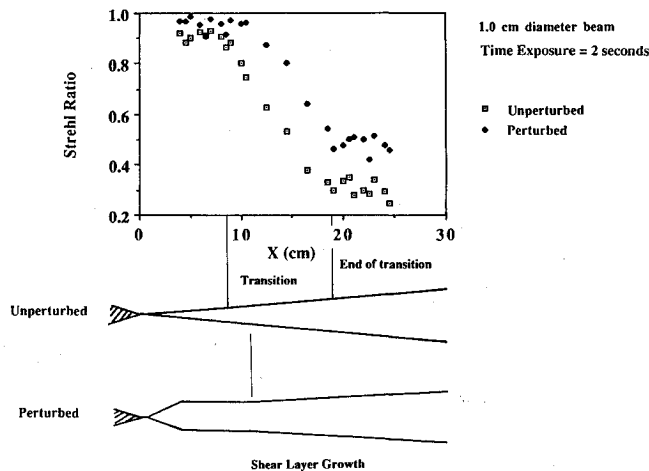


Fig. 5 Strehl ratio vs X for unperturbed and perturbed shear layers.

in size. Although this result implies that the stop in layer growth causes the Strehl ratio to remain high, it is suggested that this is only part of the reason. It is theorized that forcing a shear layer affects the shear layer more than just the growth rate of the layer. In 1985, Robert¹³ found that all additional mixing stops in this region of no growth. Although the vortices are present, there is no new entrainment and a decrease in molecular scale mixing occurs. It is therefore plausible that forcing a shear layer inhibits the growth of the number of small-scale structures. This reduction in the cascading process reduces the number of small three-dimensional vortices per unit volume existing within the shear layer, which results in less beam scattering. The combination of a reduced number of small vortices per unit volume and lack of layer growth contributes to limiting further beam degradation. The result is a constant Strehl ratio.

V. Shear-Layer Modeling

Previous models neglect the presence of coherent structures and therefore lack the physics in predicting Strehl ratios. A new model is suggested in which the influences of both fine-scale turbulence structures and larger two-dimensional coherent structures will be considered. It is believed that fine-scale structures cause phase aberrations in the manner that Sutton predicted. The larger structures cause a sinusoidal phase delay on the transmitting beam and may be modeled as a phase grating. In this paper, the interface of the shear layer is modeled as a phase plate¹⁴ and takes the form of a growing sinusoidal function

$$\Delta(x) = B(x) \sin[2\pi f_0(x)x] \quad (6)$$

where $B(x)$ is the amplitude of the sinusoidal wave and f_0 the frequency of the sine function. The effect of the interface is to cause phase delay in the shape of the interface. The intensity pattern produced by the interface may be simply modeled by using a rectangular-aperture sinusoidal phase grating (circular is much more difficult mathematically), with the transmittance function given by

$$t(x_1, y_1) = \exp\left[j \frac{m}{2} \sin(2\pi f_0 x_1)\right] \text{rect}\left(\frac{x_1}{l_x}\right) \text{rect}\left(\frac{y_1}{l_y}\right) \quad (7)$$

where m represents the peak-to-peak excursion of the phase delay,⁸ l_x and l_y are the widths of the aperture in the x_1 and y_1 direction, respectively, and f_0 is the frequency of the grating. A transmittance function describes the magnitude of the electric field that propagates through the aperture. In this example, the amplitude is 1 inside the rectangular aperture and 0 everywhere else.

For a unit magnitude plane wave propagating through a rectangular sinusoidal phase grating with transmission function $t(x, y)$, the near-field distribution of the electric field strength $U(x_1, y_1)$ immediately behind the screen will be given precisely by $t(x, y)$. The field then undergoes a Fraunhofer diffraction, resulting in a far-field distribution $U(x_0, y_0)$. The intensity of the field can be calculated by obtaining the square of the field magnitude and the Strehl ratio calculated by dividing the peak intensity of the beam with aberration to that without phase aberration.

$$\text{SR} = \left\{ \sum_{q=-\infty}^{\infty} J_q\left(\frac{m}{2}\right) \text{sinc}\left[\frac{l}{\lambda z} (x_0 - q f_0 \lambda z)\right] \text{sinc}^2\left(\frac{l y_0}{\lambda z}\right) \right\}^2 \quad (8)$$

This argument for the Strehl ratio may be numerically programmed with the correct values of phase delay $m/2$ and spatial frequency f_0 . In a medium with refractive index fluctuation, the phase excursion suffered by a coherent, incoming wave is⁸

$$\phi(x) = k(\text{OPD}) \quad (9)$$

The optical path difference (OPD) is given by

$$\begin{aligned} \text{OPD} &= \int n \, dl \\ &= \Delta(x)(n_1 - n_2) \end{aligned} \quad (10)$$

where $\Delta(x)$ is the sinusoidal interface and $(n_1 - n_2)$ is the index difference between the two streams. Because $k = 2\pi/\lambda$ and $\Delta(x) = B(x) \sin(2\pi f_0 x)$, the phase delay may be written in the following manner:

$$\begin{aligned} \phi(x) &= k(n_1 - n_2)\Delta(x) \\ &= k(n_1 - n_2)B(x) \sin(2\pi f_0 x) \end{aligned} \quad (11)$$

where $B(x)$ is the amplitude of the sinusoidal function. The peak-to-peak phase excursion m is the maximum amplitude of the foregoing function and can be written in the following form:

$$m = k(n_1 - n_2)B(x) \quad (12)$$

The experimental value of $(n_1 - n_2)$ from Table 1 is used to calculate the phase delay. The experimental δ (measured from the shadowgraphs) corresponds to the analytical amplitude $B(x)$. However, because of the variation in experimental values and the need to fit the results, a weighting factor called the phase factor ζ is introduced. The phase delay employed in this analysis can be written as

$$m = k(n_1 - n_2)\delta\zeta \quad (13)$$

By using Eq. (13), m is calculated for each shear layer at a different velocity ratio and is substituted into Eq. (8). For each X position, $f_0 = 1/\delta$ is calculated and also substituted into Eq. (8). The Strehl ratio is then numerically calculated and the results are presented in Fig. 6, which shows the Strehl ratio plotted against velocity ratio. Note how the numerically calculated values take on forms very similar to those of the experimental values. The best fit of model occurs when ζ is 0.3. This result may mean that the phase delay caused by the sinusoidal grating is not the peak-to-peak amplitude of the sine function, but instead a one-third fraction of the amplitude. As seen in the figure, this model was applied to the 6.5-cm-diam beam only; it does not apply to the 1-cm-diam beam because the beam has to pass through several vortices before the vortices can behave like a diffraction grating. If the beam size is of the same magnitude as the vortices, then no grating diffraction can occur.

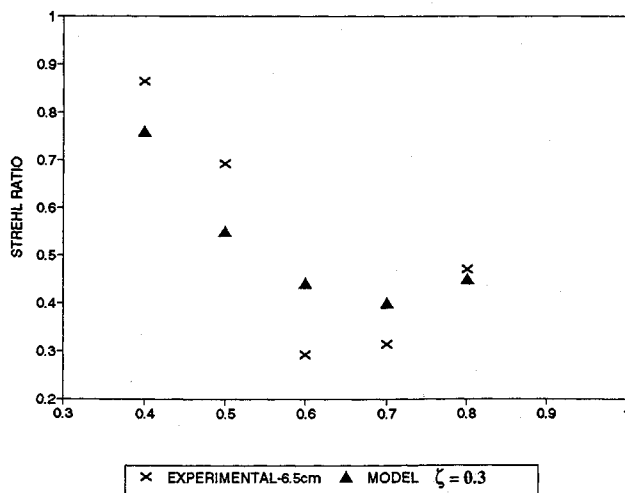


Fig. 6 Phase-plate-modeled Strehl ratio vs velocity ratio.

The results support the conjecture that the shear layer may be modeled as a phase plate with a linearly growing sinusoidal phase function. Modeling the coherent structures as a sinusoidal phase plate produces Strehl ratio values that agree well with experimental data, showing that the distribution of the vortices superimposes a sinusoidal phase delay on the beam wavefront.

VI. Summary

A wind tunnel is used to generate a low-speed shear layer between two optically dissimilar (refractive index difference) gases with a velocity ratio of 0.6 and mass density ratio of 1.0. A 6.5-cm-diam laser beam is passed through the shear layer and the time-averaged (2 s) Strehl ratio measured.

The plot of Strehl ratio vs downstream distance reveals minimal phase distortion in the pretransition region where the Strehl ratio remains constant at 0.9. When transition occurs, there is a sudden increase in the number of small-scale vortices per unit volume, which causes scattering in all directions and consequently a decrease in the Strehl ratio. Beam intensity is further reduced by the growth of the layer thickness, which increases the optical path length. In the post-transition region, the time-averaged Strehl ratio levels off to a constant asymptotic value that is a function of the velocity ratio. The constant Strehl ratio is attributed to fast mixing that occurs within the core of the vortices in the fully developed region.

Measurements in the post-transition region show that the time-averaged Strehl ratio takes on a U-shaped profile when the velocity ratio is varied from 0.4 to 0.8. Modeling the coherent structures at each of these velocity ratios as sinusoidal diffraction phase gratings produces theoretical Strehl ratios that agree well with experimental values, thereby supporting the proposed model in which large vortices behave like a sinusoidal phase plate.

Externally perturbing the shear layer alters its growth rate and the fluid mechanics of the flow in such a manner as to improve the Strehl ratio. This improvement may be attributed to the forcing function causing the vortices to be more two dimensional. It is proposed that there is an inhibition in the occurrence of smaller three-dimensional vortices. Reduction in the number of three-dimensional vortices and enhancement of the number of two-dimensional vortices reduce scattering, thereby causing the Strehl ratio to be higher.

The preceding results show that low-speed shear-layer optics are actually controlled by a combination of both the small- and fine-scale structures. Because the large scales may be controlled by external perturbation, beam propagation through low-speed shear layers may be controlled.

Acknowledgment

This work was supported by the Air Force Office of Scientific Research, whose assistance is gratefully acknowledged.

References

- Christiansen, W. H., Russell, D. A., and Hertzberg, A., "Flow Lasers," *Annual Review of Fluid Mechanics*, Vol. 7, 1975, pp. 115-139.
- Goodman, J. W., *Introduction to Fourier Optics*, McGraw-Hill, New York, 1968, pp. 57-69.
- Sutton, G. W., "Aero-optical Foundations and Applications," *AIAA Journal*, Vol. 23, No. 10, 1985, pp. 1525-1537.
- Craig, J. E., and Allen, C., "Aero-optical Turbulent Boundary Layer/Shear Layer Experiment on the KC-135 Aircraft Revisited," *Optical Engineering*, Vol. 24, No. 3, 1985, pp. 446-454.
- Chew, L., "Experimental Investigation of Free Shear-Layer Optics," Ph.D. Dissertation, Dept. of Aeronautics and Astronautics, Univ. of Washington, Seattle, WA, Aug. 1990.
- Brown, G. L., and Roshko, A., "On Density Effects and Large Structures in Turbulent Mixing Layers," *Journal of Fluid Mechanics*, Vol. 64, Pt. 4, 1984, pp. 775-816.
- Chew, L., "Coherent Structures Effects on Shear Layer Optics,"

AIAA Paper 90-0185, July 1990.

⁸Born, M., and Wolf, E., *Principles of Optics*, Pergamon, New York, 1975, pp. 463-465.

⁹Mahajan, V. N., "Strehl Ratio for Primary Aberrations in Terms of Their Aberration Variance," *Journal of the Optical Society of America*, Vol. 73, No. 6, 1983, pp. 860, 861.

¹⁰Sutton, G. W., "Effect of Turbulent Fluctuations in an Optically Active Medium," *AIAA Journal*, Vol. 7, No. 9, 1969, pp. 1737-1743.

¹¹Vu, B. T., Sutton, G. W., Theophanis, G., and Limpacher, R., "Laser Beam Degradation Through Optically Turbulent Mixing Lay-

ers," AIAA Paper 80-1414, July 1980.

¹²Koochesfahani, M. M., and Dimotakis, P. E., "Mixing and Chemical Reactions in a Turbulent Liquid Mixing Layer," *Journal of Fluid Mechanics*, Vol. 170, Sept. 1986, pp. 83-112.

¹³Robert, F. A., and Roshko, A., "Effects of Periodic Forcing on Mixing in Turbulent Shear Layers and Wakes," AIAA Paper 85-0570, March 1985.

¹⁴Tsai, Y. P., "Two-Dimensional Numerical Simulation of Free-Shear-Layer Optics," Ph.D. Dissertation, Dept. of Aeronautics and Astronautics, Univ. of Washington, Seattle, WA, 1989.

AIAA Short Course

Radar Cross Section/Stealth Technology

This short course was designed for the nonstealth specialist with sufficient descriptive material included to enable the nonengineer to grasp the essential concepts. Though the content is technical, with numerous equations and derivations of critical formulas, the emphasis of the course is an understanding of the science and technology for stealth vehicles.



American Institute of
Aeronautics and Astronautics

For additional information, contact Johnnie White, Continuing
Education Coordinator, Telephone 202/646-7447

FAX 202/646-7508